A Quantitative Analysis of the Lassen Hydrothermal System, North Central California

S. E. Ingebritsen[1] and M. L. Sorey

U. S. Geological Survey, Menlo Park, California

Our conceptual model of the Lassen system is termed a liquid-dominated hydrothermal system with a parasitic vapor-dominated zone. The essential feature of this model is that steam and steam-heated discharge at relatively high altitudes in Lassen Volcanic National Park (LVNP) and liquid discharge with high chloride concentrations at relatively low altitudes outside LVNP are both fed by an upflow of high-enthalpy two-phase fluid within the Park. Liquid flows laterally away from the upflow area toward the areas of high-chloride discharge, and steam rises through a vapor-dominated zone to feed the steam and steam-heated features. Numerical simulations show that several conditions are necessary for the development of this type of system, including (1) large-scale topographic relief; (2) an initial period of convective heating within an upflow zone followed by (3) a change in hydrologic or geologic conditions that initiates drainage of liquid from portions of the upflow zone; and (4) low-permeability barriers that inhibit the movement of cold water into the vapor zone. Simulations of thermal fluid withdrawal south of LVNP, carried out in order to determine the effects of such withdrawal on portions of the hydrothermal system within the Park, generally showed decreases in pressure and liquid saturation beneath the vapor zone which resulted in temporary increases and subsequent decreases in the rate of upflow of steam. A generalized production-injection scenario that could mitigate the effects of development on both the high-chloride and steam-fed features was identified.

Introduction

The Lassen area is in north central California, approximately 75 km east of Redding and 20–30 km northwest of Lake Almanor (Figure 1). Surficial thermal discharge features in the Lassen region are confined to the southern part of Lassen Volcanic National Park (LVNP) and the Lassen Known Geothermal Resource Area (Lassen KGRA). They include fumaroles and acid-sulfate springs at relatively high elevations in LVNP and neutral pH high-chloride hot springs at relatively low elevations in the KGRA. Although these features are widely separated, they appear to be connected to and fed by a single convection system at depth. The Lassen system is similar in this respect to other high-temperature hydrothermal systems in regions of moderate to great relief, including the Valles Caldera (Baca) system in New Mexico and the Tongonan system in the Philippines. The essential characteristic of such systems is phase separation within a zone of upflow of two-phase fluid, with steam rising to discharge at higher altitudes in areas of fumaroles and acid-sulfate springs, and high-chloride liquid flowing laterally to discharge at lower altitudes.

Such phase separation is a result of the density difference between steam and liquid water, which can cause the net forces acting on the two fluids to differ in direction as well as magnitude. In general, if permeable zones exist that allow both vertical and horizontal movement of fluids and provide outlets at different elevations, some degree of phase separation will occur. *Hubbert*'s [1953] concept of impelling force allows

[1] Also at Department of Applied Earth Sciences, Stanford University, Stanford, California.

this point to be illustrated graphically. Neglecting capillary effects,

$$\phi_w = \int_{P_0}^{P} \frac{dP}{\rho_w(P)} + gz \qquad \phi_s = \int_{P_0}^{P} \frac{dP}{\rho_s(P)} + gz$$

$$E_w = -\operatorname{grad} \phi_w \qquad E_s = -\operatorname{grad} \phi_s$$

$$= g - \frac{1}{\rho_{wr}} \operatorname{grad} P \qquad = g - \frac{1}{\rho_{sr}} \operatorname{grad} P$$

where E is the impelling force, ϕ is potential per unit mass, P is pressure, ρ is density, g is gravitational acceleration, and z is height above a datum. The subscripts w and s refer to water and steam, respectively, and the subscript r indicates reference density. Thus the impelling force is a vector quantity that defines the direction in which an element of fluid will tend to migrate.

Figure 2a depicts a high-temperature hydrothermal system in which large-scale phase separation takes place, and Figure 2b shows the forces acting on elements of steam and liquid water within the zone of two-phase upflow. The lateral component to the pressure gradient and the difference between ρ_w and ρ_s causes the impelling forces E_w and E_s to diverge. Phase separation occurs where avenues for lateral flow of liquid water exist, with liquid water tending to move laterally from (S) and steam tending to rise.

In mountainous terrain this type of phase separation may occur on a scale such that liquid water discharges in high-chloride spring areas several kilometers or more away from the main upflow zone. The phase separation process takes place on a smaller scale in high-temperature systems in gentler terrain, such as Broadlands and Wairaekei in New Zealand [*Grant, 1979; Allis, 1980*].

The generalized pressure-depth relations illustrated in Figure 2c may apply to certain hydrothermal systems in which large-scale phase separation takes place. Systems of this type have been referred to as liquid-dominated hydrothermal sys-
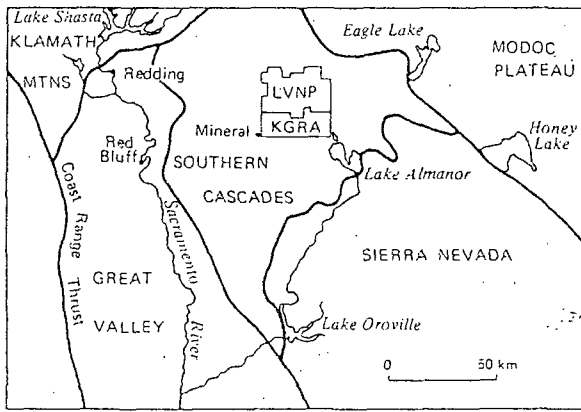
Fig. 1. Physiographic provinces in northern California and adjacent states [after *Fenneman*, 1928] and location of Lassen Volcanic National Park (LVNP) and Lassen Known Geothermal Resources Area (KGRA).

The pressure at the top of the vapor-dominated zone is nearly equal to the pressure at the base of an overlying zone of steam condensate and shallow groundwater. The maximum thickness of the vapor-dominated zone is constrained by the altitude difference between the steam and high-chloride liquid discharge areas and the pressure gradient required to drive the lateral outflow.

The conceptual model depicted in Figure 2 is consistent with the evidence discussed below regarding the nature of the Lassen hydrothermal system, although drilling in the upflow area would be required to confirm the presence and extent of distinct vapor-dominated and condensate zones. Our study of the Lassen system was based on this conceptual model and included hydrologic and geochemical field investigations and numerical simulations of heat and fluid flow. The analysis of this model applies to the evolution of the present-day Lassen system and similar systems in other areas, as well as the possible effects of fluid production for geothermal development.

GEOLOGIC SETTING

tems with parasitic vapor-dominated zones [*Sorey and Ingebritsen*, 1983a, 1983b, 1984] and as hybrid reservoirs with horizontal outflow and parasitic vapor [*Grant*, 1979]. Above the area of phase separation, steam rises through a vapor-dominated zone in which steam is the pressure-controlling phase and the vertical pressure gradient is near vaporstatic.

The Lassen area is at the southern end of the Cascade Range, which here is reduced to a broad ridge of late Pliocene and Quaternary rocks, primarily pyroxene andesite flows and pyroclastics with minor basaltic and silicic flows and pyroclas-
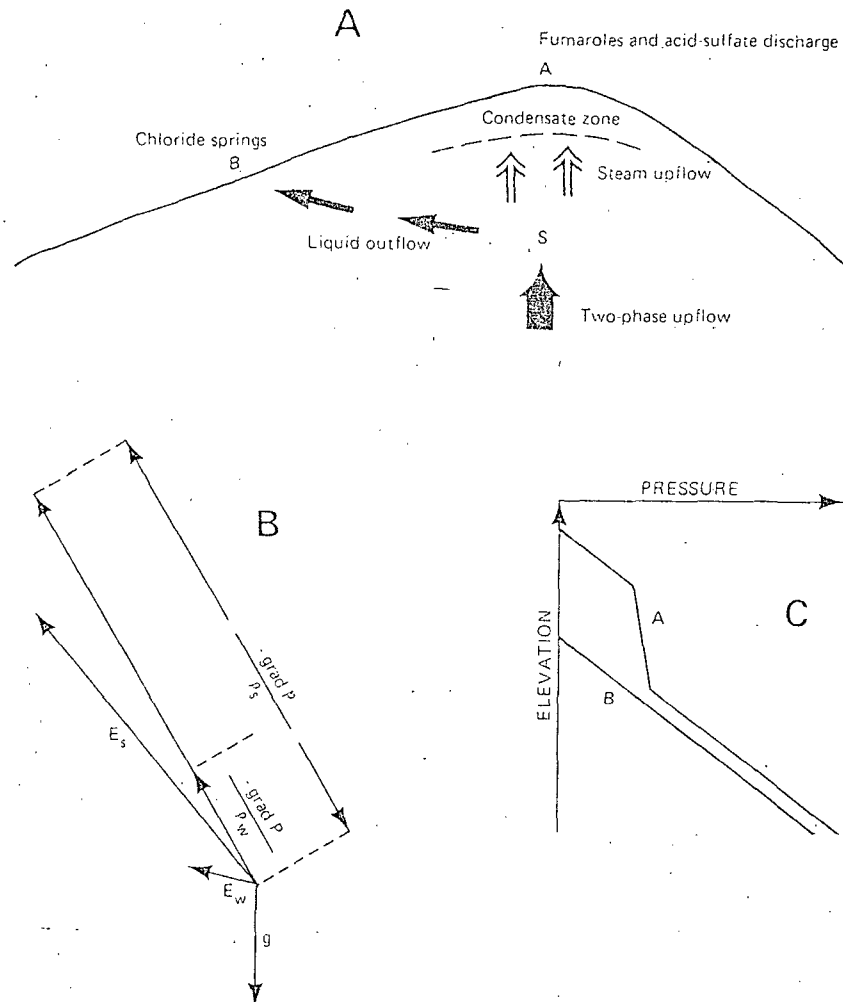

Fig. 2. (a) Schematic diagram of a high-temperature hydrothermal system in which large-scale phase separation takes place [after *Grant*, 1979]. (b) Impelling forces acting on elements of steam and liquid water in the area of phase separation (S). (c) Generalized pressure-elevation relations for liquid-dominated hydrothermal systems with parasitic vapor-dominated zones [after *Grant*, 1979].
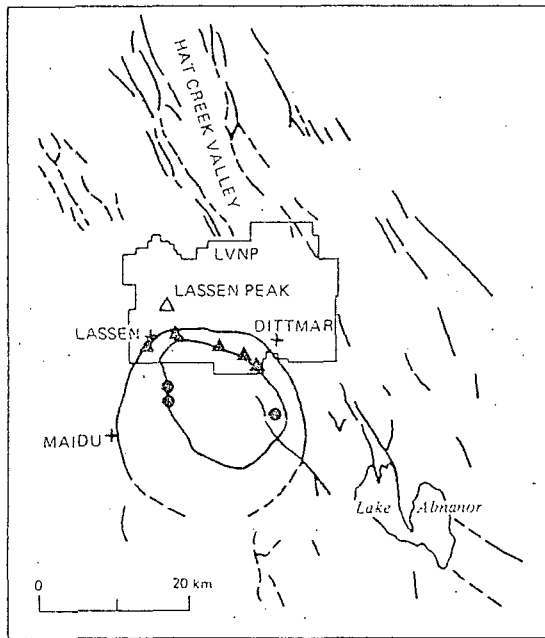
Fig. 3. Map of the Lassen region showing northwest trending structural features, ring features, major Pleistocene volcanic centers (crosses), and areas of present-day thermal fluid discharge (triangles and solid circles).

Pliocene Tuscan Formation, 'a widespread series of lahars, tuffs, and tuff breccias. Late Pliocene to Holocene volcanic rocks, of unknown thickness, overlie the Tuscan Formation in the vicinity of LVNP. Relatively high concentrations of Na, Cl, B, and NH_3 in high-chloride waters discharging in the Lassen KGRA suggest that these waters have some component that flowed through the Chico Formation [Thompson, 1983], which in turn implies a deep root to the Lassen hydrothermal system.

The dominant structural trend in the Lassen region is northwest to southeast. It is expressed by a series of normal faults with offset beginning contemporaneously with late Pliocene volcanism (Figure 3). The volcanic plateau formed by the young volcanic rocks of LVNP may fill a portion of a graben structure extending continuously from Hat Creek Valley on the north to the Lake Almanor Depression on the south [Heiken and Eichelberger, 1980]. The structural significance of the large-scale ring features outlined in Figure 3 is speculative. These features are visible on Landsat and digital terrain imagery and are defined geomorphically by valleys, drainage patterns, and other lineaments. It has been suggested that the outer ring ("Sifford Peak Depression") is the surface expression of a late Pliocene caldera [Ingebritsen and Rojstaczer, 1983; E. Rich, unpublished manuscript, 1975] or a "volcano-tectonic collapse structure" [Friedman and Frank, 1978]. All of the major thermal-fluid discharge features in the Lassen area lie on or near the "Inner Sifford Peak Ring."

Late Pliocene to Holocene volcanic rocks in the Lassen region were extruded from three long-lived volcanic centers (Figure 3): the Dittmar, Maidu, and Lassen centers [Muffler et al., 1982; Clynne, 1983]. Each of these volcanic centers evolved in three stages: (1) an initial cone-building period of andesitic lava flows and pyroclastic rocks, (2) a later cone-

tics [Muffler et al., 1982]. The regional basement probably consists of Mesozoic granitic and metamorphic rocks overlain by a thin sequence of marine rocks of the Late Cretaceous Chico Formation. The Late Cretaceous rocks are probably overlain by the Eocene Montgomery Creek Formation, a series of sandstones, conglomerate, and shales, and by the late
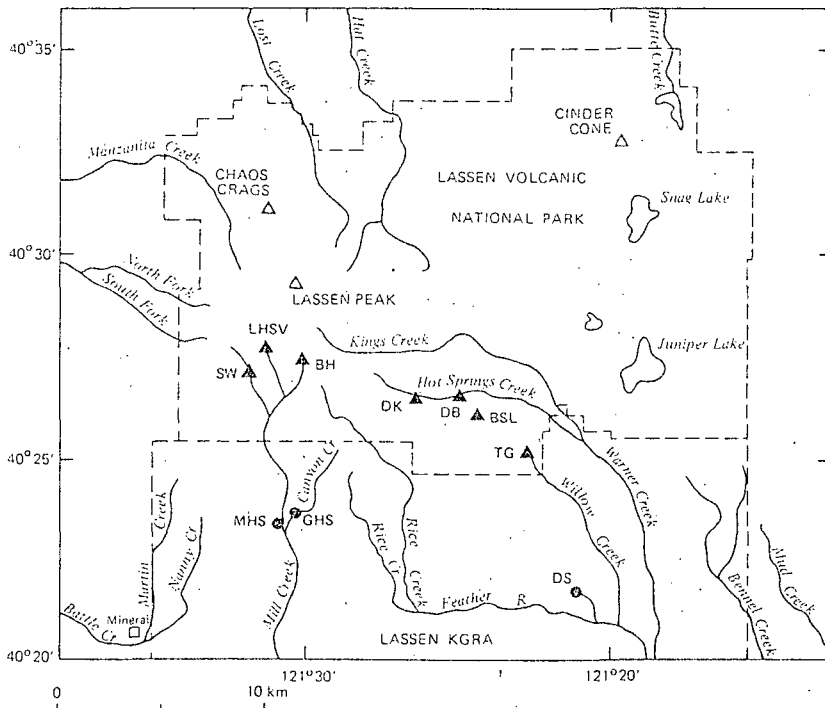

Fig. 4. Map showing areas of thermal fluid discharge and major streams in the Lassen region. Areas with fumaroles, steam-heated springs, and/or low-chloride conductively heated springs are shown as triangles (BH, Bumpass Hell; LHSV, Little Hot Springs Valley, SW, Sulphur Works; DK, Devils Kitchen; DB, Drakesbad; BSL, Boiling Springs Lake; TG, Terminal Geyser). Areas with high-chloride thermal water discharge are shown as solid circles (DS, Domingo Spring; GHS, Growler Hot Spring; MHS, Morgan Hot Springs).

TABLE 1. Typical Concentrations of Selected Ions in Thermal Waters in Lassen Volcanic National Park and Lassen KGRA

Location	Temperature, °C	pH	SO_4, mg/L	SiO_2, mg/L	Na, mg/L	Cl, mg/L	B, mg/L
Bumpass Hell	53–93	2.2	400	96–236	4–33	2–6	1
Sulphur Works	83–93	1.9–7.2	940	39–213	3–70	1–3	1–4
Little Hot Springs Valley	55–93	3.8–6.8	101–517	84–172	55–102	1–6	0.1–5.1
Devils Kitchen	71–95	1.9–7.0	226	40–213	2–43	0.5–1.6	0.3–2.4
Drakesbad	65	6.7	140	143	43	2.0	1.0
Boiling Springs Lake	94	2	710	242	6.4	13	1.6
Terminal Geyser	93	5.0	16–52	30–64	7.5	3–26	1.5
Morgan Hot Springs	82–95	7.2	110	150–184	1300	2210	80
Growler Hot Springs	95	8.0	90	250	1400	2320	95
Walker "O" No. 1 Well	86*	7.4	81	133	1220	2180	62
Domingo Spring	10	7.0	2	40	12	21	0.6

Data from *Thompson* [1983], except for the Walker "O" No. 1 well (from J. M. Thompson, unpublished manuscript, 1983).
*Temperature of surface sample. Subsurface temperature of production zone = 176°C [*Beale*, 1981].

building period of thick siliceous andesitic lava flows, and (3) eruption of dacitic to rhyolitic domes and flows on the flanks of the main composite cone. The residual silicic magma chamber associated with the third stage of the Lassen volcanic center (0.25 m.y. to present) provides the heat source for the present-day Lassen hydrothermal system.

GEOCHEMICAL CHARACTERISTICS

Figure 4 shows the locations of the thermal-fluid discharge features in the Lassen area, and typical concentrations of selected ions in the thermal waters are listed in Table 1. The generally acidic, low-chloride character of the surficial discharge features at relatively high altitudes within LVNP indicates some degree of vapor-dominated conditions at depth. High-chloride thermal water discharges at lower altitudes at Growler Hot Spring along Canyon Creek and at Morgan Hot Springs along Mill Creek and has been detected in an aquifer at depths near 500 m in the Walker "O" No. 1 well drilled at Terminal Geyser [*Beall*, 1981]. Some or all of the high-chloride water flowing under Terminal Geyser may eventually discharge at Domingo Spring, where chloride concentrations are five to ten times higher than in other cold springs in the Lassen area [*Thompson*, 1983].

Studies of gas composition [*Janik et al.*, 1983], geothermometry [*Thompson*, 1983; *Nehring et al.*, 1979], and stable isotope composition [*Janik et al.*, 1983] suggest that thermal fluids in the Lassen region circulate outward from a common upflow zone beneath Bumpass Hell. The composition of gas in steam discharging from various thermal areas shows depletion of H_2S and an increase in the proportion of CO_2 and N with increasing distance from Bumpass Hell. On this basis *Janik et al.* [1983] inferred that the thermal features between Devils Kitchen and Terminal Geyser and at Growler and Morgan Hot Springs are connected to the vapor-dominated area under Bumpass Hell by liquid-dominated lateral flow zones. The thermal aquifer intercepted by the Walker "O" No. 1 well beneath Terminal Geyser (Figure 5) is such a lateral flow zone.

Waters from the high-chloride sources yield cation and sulfate geothermometer temperatures between 212° and 235°C [*Thompson*, 1983; *Nehring et al.*, 1982]. Lower estimates from the quartz geothermometer suggest some degree of silica deposition and/or mixing with near-surface waters. Superheated

steam temperatures of up to 159°C were measured in the Big Boiler fumarole at Bumpass Hell during the California drought of 1976–1977. *Muffler et al.* [1982] point out that this temperature is close to the temperature (163°C) of steam decompressed adiabatically from saturated steam at maximum enthalpy (235° and 31 bars) to a land surface pressure of less than 1 bar. A similar steam temperature of 244°C was calculated by *Muffler et al.*, [1982] using the gas geothermometer of *D'Amore and Panichi* [1980]. The inferred temperature of the underlying steam source is thus similar to the cation and sulfate geothermometer temperatures calculated for the high-chloride waters.

Further evidence for a common source for these fluids is provided by stable isotope concentrations [*Janik et al.*, 1983]. As is shown in Figure 6, the thermal water issuing from Growler Hot Spring has a deuterium value similar to those for meteoric waters on the composite cone of the Lassen volcanic center ($SD = -95\%$) and exhibits an oxygen isotope shift of about $+4\%$, probably owing to water-rock interaction at high temperature. The isotopic content of condensed steam from Big Boiler is very similar to that calculated for steam in equilibrium with the Growler Hot Spring water at 235°C, as is
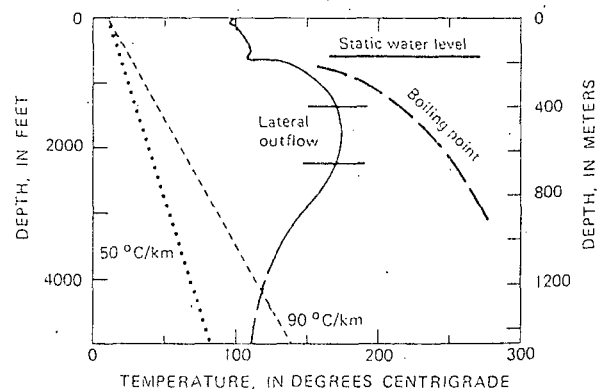
Fig. 5. Measured temperature profile (solid curve) in Walker "O" No. 1 well at Terminal Geyser showing position of the inferred lateral outflow conduit and the boiling point curve referenced to static water level. Position of the static water level is based on unpublished data from Eureka Resources (1983).
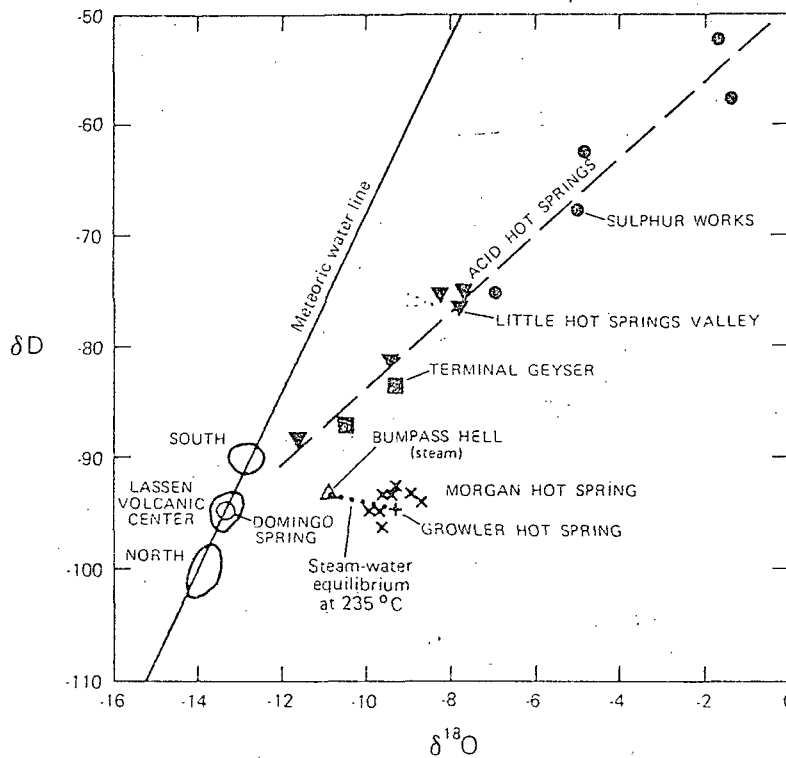
Fig. 6. Diagram showing the relationship between deuterium (D) and ^{18}O for water and steam samples from the Lassen region [adapted from *Muffler et al.*, 1983; *Janik et al.*, 1983]. Data for cold waters from the Lassen volcanic center and areas to the north and south of the Lassen volcanic center fall within the areas outlined along the meteoric water line.

indicated by the dotted line in Figure 6. Slightly lighter values of ^{18}O in waters toward the southern end of the Morgan Hot Spring area suggest dilution of this thermal water with local nonthermal groundwater.

GEOPHYSICAL CHARACTERISTICS

The geophysical setting in the Lassen region is characterized by a large gravity low centered in the northeast-

ern part of LVNP, magnetic anomalies centered over various volcanic vents, low heat flow northward from LVNP and variable heat flow within LVNP and the Lassen KGRA, and continuing seismicity of moderate magnitude. Published electrical surveys and heat flow measurements offer the most direct information regarding the Lassen hydrothermal system but have thus far been restricted to the more accessible areas in the southernmost part of the Park (audiomagnetotelluric
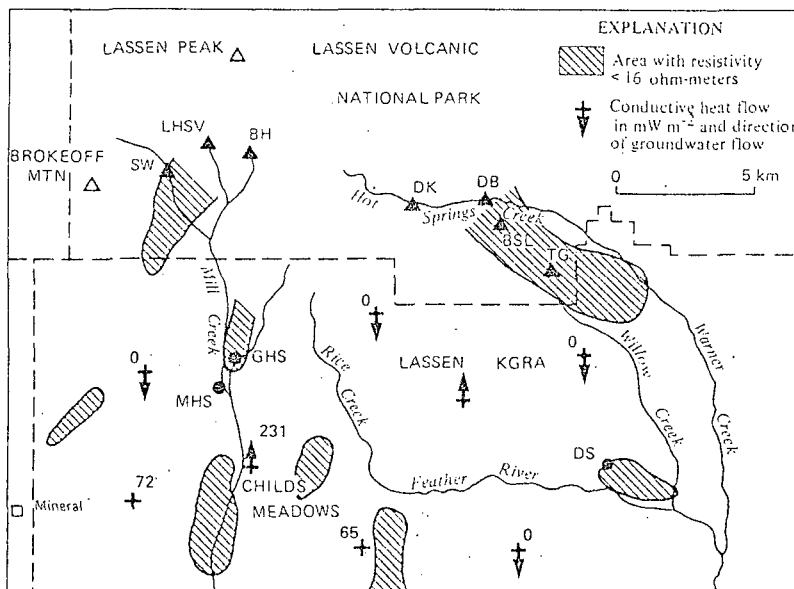

Fig. 7. Map showing areas of apparent resistivity less than 16 ohm meters, based on a 27 Hz AMT map [adapted from *Christopherson and Pringle*, 1981] and measured heat flow [*Mase et al.*, 1980]. Areas of thermal-fluid discharge are shown as triangles within LVNP and as solid circles within Lassen KGRA (see Figure 4 for explanation of abbreviations used).
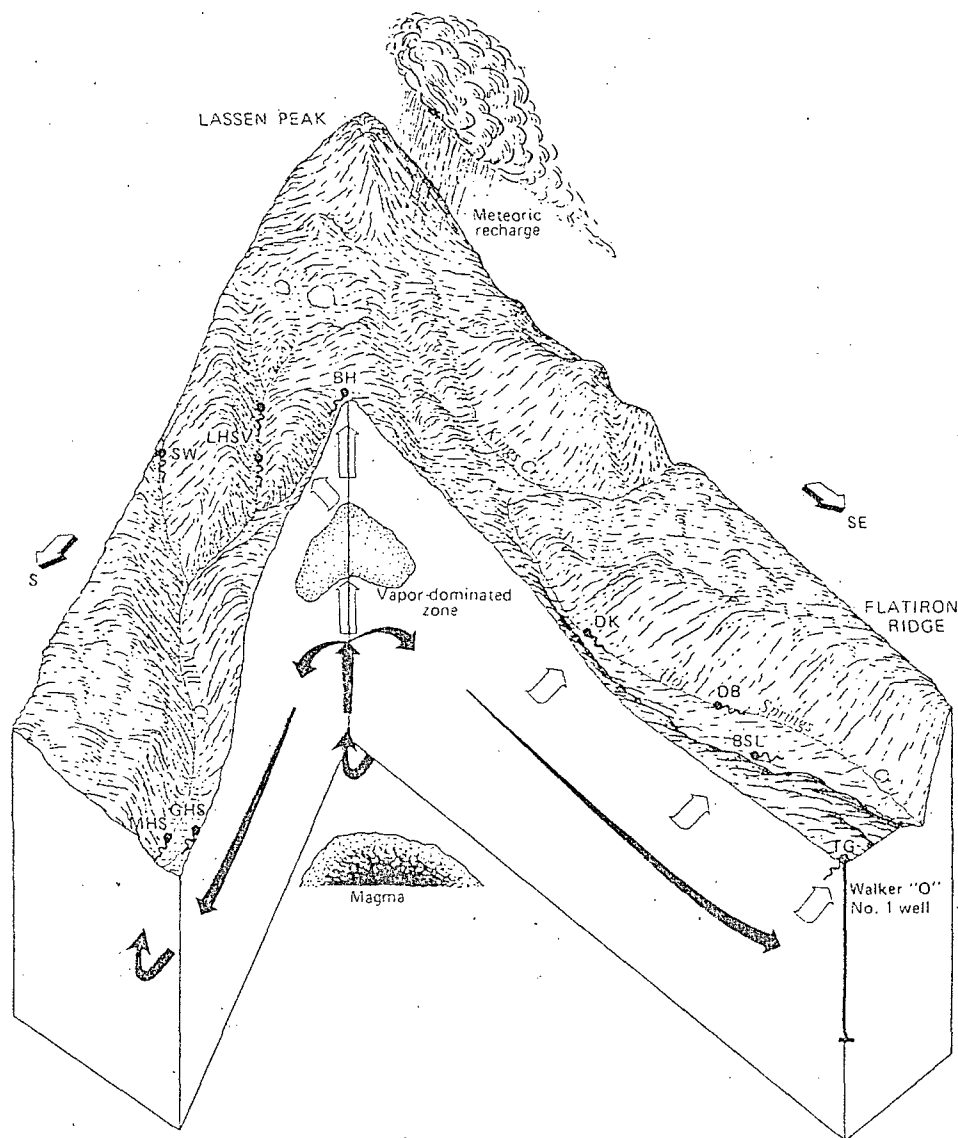
Fig. 8. Conceptual model of the Lassen hydrothermal system showing recharge from meteoric waters around Lassen Peak, upflow of heated water beneath Bumpass Hell, and phase separation with steam rising through a parasitic vapor-dominated zone and liquid flowing laterally to the south toward hot springs along Mill Creek and Canyon Creek and to the southeast past Terminal Geysers. Vertical exaggeration is approximately five times (see Figure 4 for explanation of abbreviations used).

(AMT) surveys) and the Lassen KGRA (AMT surveys and heat-flow measurements).

Relevant electrical data are contained in AMT maps at 7.5 and 27 Hz [Christopherson and Pringle, 1981]. At 7.5 Hz the depth of penetration ranges from 600–2000 m and at 27 Hz it is about half as deep, depending on the resistance of the material. Areas of resistivity less than 16 ohm meters are inferred to be underlain by thermal waters and/or hydrothermally altered rock. There are at least two such areas of low resistivity within LVNP that are suggestive of lateral flow of thermal water southward from Sulphur Works and southeastward from Drakesbad (Figure 7). Within the KGRA, the low-resistivity zones south of Morgan Hot Springs, which are also discernable on the 7.5-Hz map, may be caused by water moving southward in aquifers at depths within those penetrated by these surveys. The AMT data show no evidence of high-temperature, high-chloride water underlying the central part of the Lassen KGRA. The network of AMT stations did

not extend north of a line between Brokeoff Mountain and Drakesbad.

Mase et al. [1980] presented temperature profiles and calculated heat flows for nine shallow drillholes in the Lassen KGRA. Hole locations and heat-flow values are plotted in Figure 7. Conductive gradients from two of the holes were interpreted to represent a regional heat flow of 65–75 milliwatts per square meter (mW m^{-2}). Downward arrows, shown for five of the holes drilled near topographic highs, signify that the measured gradients were affected by groundwater downflow. Upward arrows, shown for two of the holes drilled in topographic lows, signify that the gradients were affected by groundwater upflow. In one of the latter two holes, drilled to a depth of about 200 m at the northern end of Childs Meadows, the convective disturbance is minimal and the average gradient and conductive heat flow are near 90°C/km and 230 mW m^{-2}, respectively. This anomalously large heat flow may be caused by thermal water flowing southward in an aquifer at

depths greater than 200 m beneath Mill Creek or Childs Meadows.

CONCEPTUAL AND NUMERICAL MODELS

The evidence discussed above is consistent with a conceptual model of the Lassen system that involves recharge of meteoric water on the composite cone of the Lassen volcanic center, addition of heat to this fluid by conduction from a residual silicic magma chamber and possibly from small amounts of magmatic steam, and upwelling of high-enthalpy fluid within a central upflow zone (Figure 8). Avenues of permeability for this upflow may be associated with contact zones between the andesitic rocks of the composite cone of the Lassen volcanic center and younger dacitic rocks of its third stage. The discharge of steam and acid-sulfate waters from the adjacent thermal areas at Bumpass Hell, Little Hot Springs Valley, and Sulphur Works may be fed by an areally extensive zone of upflow beneath the region encompassing these features or by shallow conduits connecting one or more of these areas to a less extensive zone of upflow.

In this model, lateral outflow to the south and southeast from the central upflow zone feeds the various surficial hydrothermal features at lower altitudes. The available data suggest that areally restricted zones of lateral flow are oriented between the central upflow zone beneath Bumpass Hell and the Growler-Morgan Hot Springs area and between Bumpass Hell and the Terminal Geyser area. Thermal discharge features are confined to these orientations, and the resistivity data from the Lassen KGRA and the southernmost part of LVNP (Figure 7) are also consistent with this interpretation. Existing data also support the extension of the Bumpass Hell to Terminal Geyser flow zone to Domingo Spring.

Although the geometry of permeable conduits within these two lateral flow zones has not yet been delineated, some degree of structural control of permeability is suggested by the apparently limited areal extent of each outflow zone and by overlying topographic lows that may be related to older buried faults. Along the southeastern trending outflow zone, two young normal faults ("Hot Springs Creek Fault" and "Terminal Geyser Fault"; Clynne [1983]) connect the thermal features at Devil's Kitchen, Drakesbad, and Terminal Geyser. Along the southward trending outflow zone, hot spring discharge along Mill and Canyon Creeks occurs near the base of the volcanic rocks derived from the Lassen volcanic center, near the contact with older rocks derived from the Maidu Volcanic Center, suggesting that the southward outflow may be related to this contact zone.

Quantitative constraints on this model of the Lassen hydrothermal system are few. Calculations based on liquid and gas geothermometry and on the thermodynamic analysis of superheated steam suggest that phase separation takes place beneath Bumpass Hell at pressures of 31–34 bars and temperatures of 235–240°C. If the region between the land surface and this zone of phase separation is liquid saturated or nearly saturated with a mixture of steam condensate and shallow groundwater, pressures would follow hydrostatic boiling point-depth relations from the land surface. This would imply phase separation at a depth of about 350 m and an altitude of 2150 m. This altitude may represent the top of a vapor-dominated zone. The altitudes of the hot springs in Mill Creek Canyon are near 1550 m, so the maximum thickness of the inferred vapor-dominated zone would be approximately 600 m. The minimum thickness of the vapor-dominated zone is unconstrained. Temperatures in the lateral flow conduits decrease away from the upflow zone owing to conductive heat loss. The amount of heat lost is affected by fluid flow rates, the depth of the conduits, and the length of time lateral flow has been taking place. Between Bumpass Hell and Terminal Geyser, temperatures in the lateral flow conduit apparently decrease from approximately 240°C to 176°C, while the temperature decrease between Bumpass Hell and Growler and Morgan Hot Springs is such that conduit temperatures beneath the hot springs are greater than or equal to the measured spring temperatures (≥ 95°C).

Additional constraints that allowed us to obtain estimates of the hydraulic properties of conduits for lateral and vertical flow from our numerical simulations were provided by measurements of the rate of discharge of thermal water at the land surface. These measurements are discussed in greater detail in the work by Sorey and Ingebritsen [1984]. Briefly, Mill and Canyon Creeks were gaged and sampled both upstream and downstream from the Growler and Morgan Hot Springs areas. The chloride flux at each measurement site was calculated as the product of stream flow and chloride concentration. The upstream chloride concentration was below measurable limits, so the contribution of thermal water from hot spring orifices and streambed seepage could be estimated as the total chloride flux below the hot spring areas divided by the chloride concentration of the hot spring waters (Table 1). The chloride flux measurements indicated that the total flow of thermal water discharging at the surface along Mill and Canyon Creeks is approximately 17 kg/s. This figure probably represents most of the lateral flow along the Bumpass Hell to Growler and Morgan Hot Springs orientation. However, the anomalously high heat flow value and the low resistivity values south of Morgan Hot Springs (Figure 7) suggest that an unknown amount of thermal fluid flows past the hot spring areas in the subsurface. Some of the thermal fluid flowing under Terminal Geyser may eventually discharge at Domingo Spring, where chloride flux measurements indicate a thermal component of approximately 2.7 kg/s. Fluid discharge from areas of fumaroles and acid-sulfate springs within LVNP is more difficult to quantify, but may be at least an order of magnitude less than the mass flow of high-chloride water [Sorey and Ingebritsen, 1984].

A schematic cross section of the Bumpass Hell to Growler and Morgan Hot Springs flow axis is shown in Figure 9a. Numerical simulations of heat and fluid flow within the Lassen system were carried out using a geometric model corresponding to this flow axis (Figure 9b), from which the discharge of high-chloride water is reasonably well constrained. With reference to Figure 9a, the numerical model is restricted to the regions of upflow and lateral outflow and does not include the recharge area or the region of magmatic heating. A two-dimensional model was chosen in part because of the computational difficulties and expense involved in three-dimensional simulations of multiphase flow over geologic time periods. Inclusion of the southeastward trending axis in the model would have added useful constraints provided by the known temperature and elevation of the lateral conduit beneath Terminal Geyser. However, excluding this part of the flow system saves considerably on computational requirements and should not alter the basic conclusions derived from these simulations.

The geometric model consists of a vertical slab of uniform width with a sloping upper boundary representing land-surface elevations between Bumpass Hell and Growler and Morgan Hot Springs. Fluid circulation within this model is
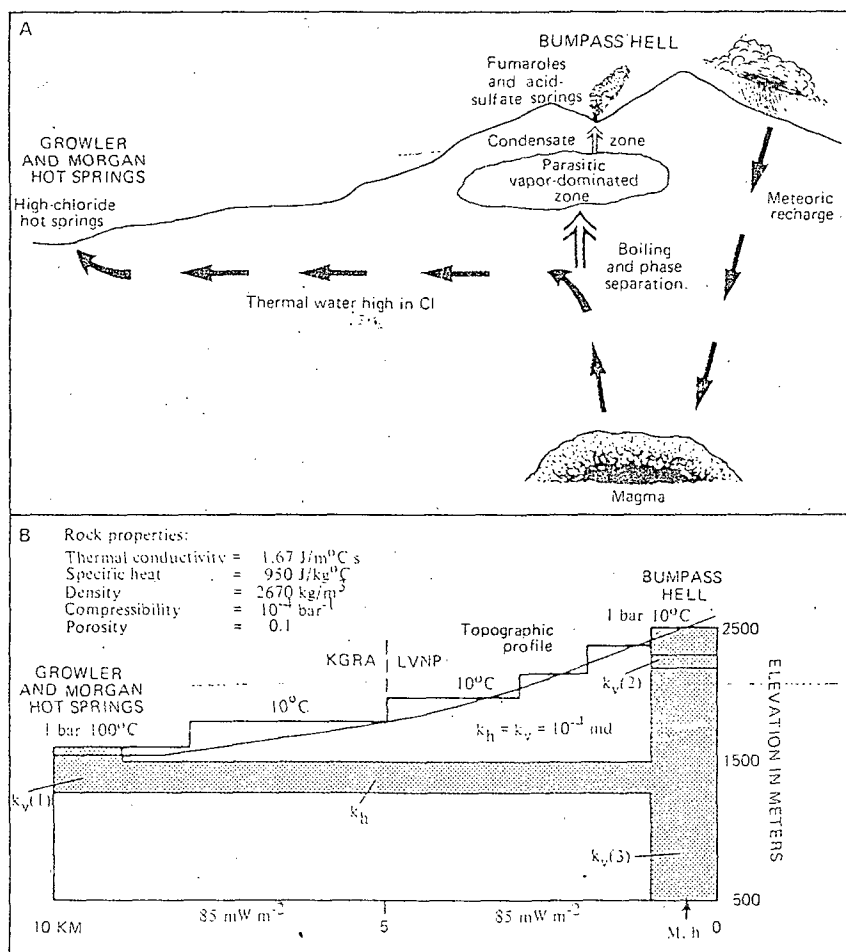
Fig. 9.   (a) Schematic cross section of the Bumpass Hell, Growler, and Morgan Hot Springs orientation of the Lassen hydrothermal system [adapted from *Muffler et al.*, 1983]. (b) Geometric model used in simulations of the Lassen hydrothermal system. Arrow indicates inflow of hot water with mass flow rate M and enthalpy h. Fluid flow is essentially confined to regions shown with dotted pattern. Horizontal and vertical intrinsic permeabilities indicated by symbols k_h and k_v, respectively.

essentially confined to the vertical conduits along the sides and the lateral conduit, which for simplicity is assumed to be a horizontal stratum 200 m in thickness, with its base at an elevation of 1300 m. Constraints provided by the estimated phase-separation pressure of 31–34 bars and by the need for a pressure gradient sufficient to drive the lateral outflow indicate that the lowest possible elevation for the base of such a conduit is about 1200 m, whether the conduit is horizontal or sloping. Circulation is driven by a specified mass inflow of hot water at the lower right, and discharge occurs at the upper right and left sides of the model. Along the base, a conductive heat flux of 85 mW m^{-2} is specified to represent the regional flow.

The model width is 1 km, a value close to the average width of the glacially eroded Mill Creek Canyon. As is noted above, the lateral conduit could represent a stratigraphic unit, such as a contact zone between different flow rocks, or a zone of weakness associated with a structurally controlled fracture or fault zone. The actual conduit could be thinner but more areally extensive than assumed here. Results from the numerical simulations depend to some extent on the conduit geometry used in the model, as is discussed below.

A 10 by 13 array of variably spaced grid blocks was utilized for numerical simulations of heat and fluid flow in the model. This yielded an approximation to the actual land-surface to-

pography, as is shown in Figure 9b. The computer code used was a modified version of the three-dimensional, two-phase fluid and heat transport program described by *Faust and Mercer* [1979]. With this program, solutions for fluid pressure and enthalpy at selected times are obtained using finite-difference techniques. Other system properties such as liquid-steam saturation and rock-fluid temperature are obtained from the calculated pressures and enthalpies. Modifications to the original code were made to improve the scheme for up-stream weighting of fluid properties and relative permeabilities and to allow conductive heat flux to be specified as a boundary condition [*Ingebritsen*, 1983]. Numerical simulations of the evolution of the Lassen system were made more difficult by the need for relatively small time steps during periods of transition from single- to two-phase flow within total simulation times on the order of 10,000 years.

EVOLUTION SIMULATIONS

Simulations of the evolution of the Lassen hydrothermal system provided insight into the conditions required for the development of such systems in general, as well as estimates of the rock properties and boundary conditions controlling heat and fluid flow in the Lassen system itself. In the absence of adequate drillhole data, the evolution simulations were used to generate estimates of parameter values. Combinations of
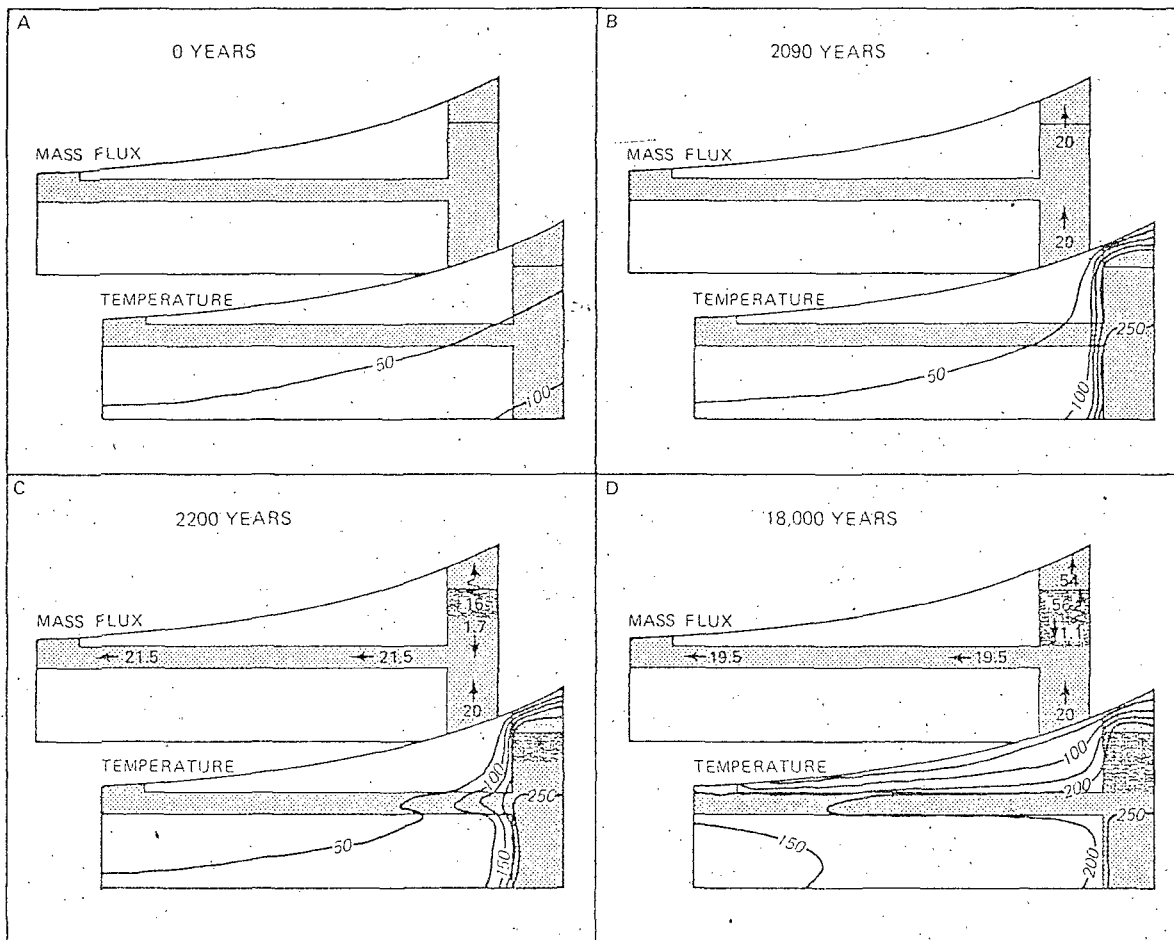
Fig. 10. Mass flow vectors (straight arrows for liquid, curved arrows for steam) and temperature distributions at selected times during evolution of a liquid-dominated hydrothermal system with a parasitic vapor-dominated zone. Permeability of the lateral conduit was increased from 1.0×10^{-4} to 140 md at a simulation time of 2090 years. Dotted pattern represents the region of vapor-dominated conditions.

parameters that allowed the evolution of the system to be simulated successfully were regarded as reasonable estimates. The initial pressure and enthalpy conditions for simulations of geothermal development were based on the results of the evolution simulations.

Evolution Processes

Our simulations indicated that several conditions are necessary for the development of Lassen-like systems. These include moderate to great topographic relief, which allows large-scale phase separation; an initial period of convective heating within an upflow zone followed by some change in hydrologic or geologic conditions that initiates drainage of liquid from portions of the upflow zone; and low-permeability barriers that inhibit the movement of cold waters into the vapor zone.

Evolution of the Lassen hydrothermal system is likely to have begun with a period in which mineralized hot water discharged at the land surface above the main region of upflow. Fossil sinter remnants in the Devils Kitchen area (L. J. P. Muffler, personal communication, 1983) and in the Mud Volcanoes area of Yellowstone National Park [*White et al.,* 1971] provide evidence that high-chloride waters once discharged in certain areas now characterized by acid-sulfate discharge. During this early period, rock-fluid temperatures in the upflow zone would have increased to levels such that two-phase conditions could develop if pressures were subsequently

reduced. At the same time, deposition of silicate and carbonate minerals at shallow depths may have occurred to a degree sufficient to produce an aureole of relatively low permeability. Such a feature is necessary to restrict inflow of cooler water during the depressurization and draining of liquid that accompanies the development of a vapor zone.

A parasitic vapor-dominated zone can develop within low-permeability barriers by several mechanisms that initiate a reversal in the direction of liquid flow, allowing water to drain from beneath a low-permeability caprock as pressures are lowered to saturation levels and steam replaces liquid. Associated with each mechanism is lateral flow of thermal water away from the upflow zone toward discharge areas at lower altitudes. For drainage to occur, the rate of outflow in the lateral conduit must exceed the rate of mass inflow to the system for some period of time.

Mechanisms considered in this study for inducing such a drainage process included (1) an increase in the permeability of a fault-controlled lateral conduit or the channel connecting it to the high-chloride spring outlet, due, for example, to seismic activity; (2) a decrease in the rate of inflow (recharge) to a value less than the flow rate established in the lateral conduit; (3) a lowering of the altitude of the hot spring outlet, causing an increase in the lateral pressure gradient; and (4) a gradual decrease in fluid viscosity as hot water flowing away from the upflow zone heats up the lateral conduit. Each of these mecha-
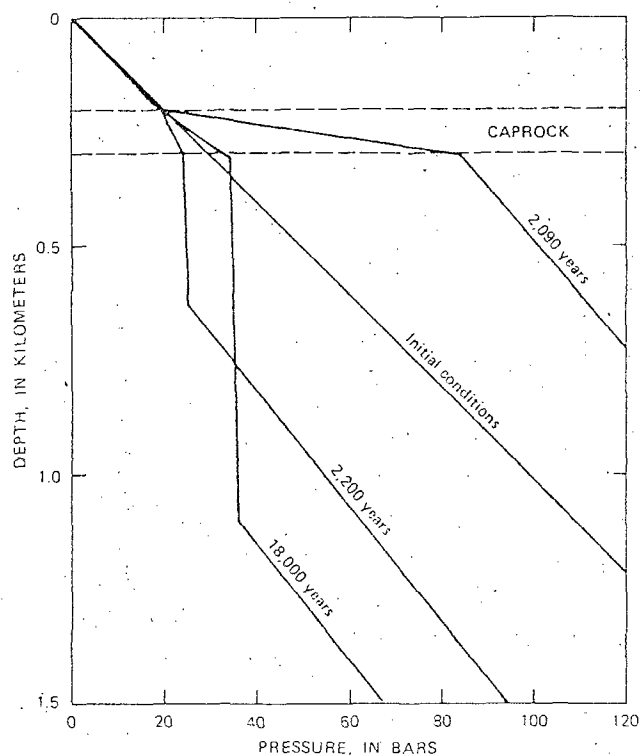
Fig. 11. Pressure profiles in the upflow column during evolution of a liquid-dominated hydrothermal system with a parasitic vapor-dominated zone. Profiles shown for selected times since upflow begins for a case in which lateral flow is initiated at 2090 years by increasing the permeability of the lateral conduit.

$k_v(1) = 100 \text{ md} = 1 \times 10^{-9} \text{ cm}^2$;
$k_c(2) = 0.05 \text{ md}$;
$k_v(3) = 100 \text{ md}$;
$k_{rl} = [(S - 0.3)/0.65]^4$;
$k_{rs} = [1 - (S - 0.3)/0.65]^2 \times [(1 - (S - 0.3)^2)/0.4225]$.

where k_{rl} and k_{rs} are Corey-type functions for steam and liquid relative permeabilities, S is liquid saturation, and the other terms are defined in Figure 9b. The initial temperature distribution corresponds to a uniform conductive heat input of 85 MW m^{-2}, and the initial pressures vary hydrostatically with depth (Figures 10a and 11).

The upper part of the upflow conduit below the caprock layer is heated to temperatures of more than 200°C during the initial period of upflow with no lateral flow. One hundred and ten years after lateral flow is initiated due to the increase in k_h (Figure 10c), a vapor-dominated zone has begun to develop beneath the caprock layer as liquid drains toward the lateral conduit. The corresponding pressure distribution in this region is close to vaporstatic, with pressures controlled mainly by the temperatures prevailing when drainage commences. Drainage continues for another 1400 years until the vapor-dominated zone extends to the top of the lateral conduit. Subsequently, steam pressures slowly increase as liquid saturation decreases in the underlying two-phase region, and the rate of steam upflow increases. Final pressures in the vapor zone in this case are near 34 bars. Temperatures in the lateral conduit increase slowly throughout the simulation as the hot water front moves toward the low-elevation end of the model. Approximately 18,000 years are required for temperatures near the discharge end to rise to quasi steady state values of about 170°C (Figure 10d).

Mass flow vectors at quasi steady state (Figure 10d) indicate a counterflow of liquid and steam within the vapor-dominated zone, with a net upflow of 0.54 kg/s. At the base of the caprock layer, some steam condenses and flows downward while the remainder flows into the caprock layer, where it condenses before rising to the land surface. The mass flux of liquid across the land surface represents the discharge of steam and steam condensate above the central upflow area and is equivalent to the net mass upflow of steam through the vapor zone. Real world complications involving separate channels for steam and liquid within the condensate zone are neglected in this model. Note that in this simulation the net rate of upflow through the vapor and condensate zones is only about 3% of the lateral outflow rate. As is discussed below, several factors influence the ratio of steam upflow to lateral outflow, including the mass inflow rate and enthalpy, the permeability of the caprock, and the form of the relative permeability functions.

The temperature distribution above and below the lateral conduit (Figure 10d) shows the effects of conductive heat loss from the lense of hot water in the conduit. The time required to reach quasi steady state is controlled mainly by the lateral flow velocities and the thickness and thermal conductivity of the rock above the conduit. The greater the average velocity, the shorter the equilibration time, and the higher the resultant quasi steady state temperatures along the conduit. For example, decreasing the inflow rate M from 20 kg/s to 10 kg/s changes the average lateral velocity by roughly the same factor and results in an equilibration time of 23,000 years and a conduit temperature at the left side of the model of about 100°C [Ingebritsen, 1983]. If the average lateral velocity were halved by doubling the cross-sectional area of the conduit

nisms appears geologically or hydrologically plausible, but one or more could be considered more likely to have occurred in specific systems of this type.

Numerical simulations were continued until the pressure distribution reached conditions similar to those in Figure 2c, with pressures in the 31–34 bar range in the vapor-dominated zone, and temperatures in the lateral conduit had become relatively stable (changing less than 1°C per 1000 years). The desired temperature and pressure distributions in the lateral conduit at this quasi steady state condition were constrained only by the requirement that conduit temperatures at the left side of the model be above the surface boiling point of 95°C. Factors affecting the simulated end point conditions include the mass inflow rate M, inflow enthalpy h, horizontal and vertical permeabilities k_h and k_v, and the relative permeability-liquid saturation functions. The complex interactions between thermodynamic and hydraulic processes in these simulations made considerable experimentation necessary to identify the required combinations of parameter values.

Results

Typical results of simulations of the evolution of the Lassen hydrothermal system are shown in Figures 10 and 11, for a case in which mechanism (1) was invoked after approximately 2100 years of upflow with no lateral flow. At this point the permeability of the lateral conduit was increased from 0.0001 to 140 md. Values of other parameters used in this simulation are as follows:

$M = 20$ kg/s;
$h = 1125$ J/g (258°C at 101 bars);

while keeping $M = 20$ kg/s, similar effects on the equilibration time and conduit temperature would have been observed.

Travel times for fluid flow between the upflow zone and the discharge end of the model under quasi steady state conditions can be calculated from the equation

$$t = \frac{A\bar{\rho}Ln}{Q}$$

where t is the travel time in the lateral conduit, A is the cross-sectional area of the conduit, $\bar{\rho}$ is the average fluid density, L is the length of the conduit, n is the conduit porosity (0.1 in all simulations), and Q is the mass flow rate in the conduit (approximately equal to the inflow rate M). For $M = 20$ kg/s, $t = 240$ years, and for $M = 10$ kg/s, $t = 500$ years.

One particularly useful result of our evolution simulations was the delineation of a relatively narrow range of possible values for the permeability–cross–sectional area product of the southward trending lateral flow conduit. The necessary constraints were provided by the estimated phase-separation pressure of 31–34 bars and by the estimate from chloride flux measurements of approximately 20 kg/s for the total mass flow rate. Simulations that yielded quasi steady state conditions matching these constraints provided estimates of k_h applicable to the conduit geometry used in the model. For the simulation illustrated in Figures 10 and 11, the value of k_h is 140 md.

Additional factors influencing the determination of conduit permeability are the possible presence of liquid-dominated two-phase conditions in the conduit away (downstream) from the upflow zone and the value of vertical permeability below the hot-spring discharge boundary ($k_v(1)$). For the quasi steady state result illustrated in Figure 10d, two-phase flow extends about 4 km downstream from the upflow zone, and within this region the relative permeability to liquid averages about 0.35. Additional simulations with a much lower value of vertical permeability below the hot spring discharge boundary ($k_v(1)) = 0.6$ md versus $k_v(1) = 100$ md) resulted in higher pressures and a reduced pressure gradient within the lateral conduit, and the absence of two-phase flow except immediately below the vapor-dominated zone. Fortuitously, the resulting combination of greater relative permeability to liquid and smaller pressure gradient is such that the value of k_h required to transmit the mass flow rate is only slightly greater (180 md). The presence or absence of an extensive liquid-dominated two-phase region in the lateral conduit would have a strong influence on the rate of propagation of pressure changes induced by fluid withdrawal for geothermal development and is therefore an important feature of the Lassen hydrothermal system yet to be delineated.

The simulated net rate of upflow of steam within the vapor-dominated zone under quasi steady state conditions depends primarily on the value of caprock permeability ($k_v(2)$). Steam upflow increases as the caprock permeability is made greater. For example, the net upflow rate at quasi steady state for the simulation illustrated in Figure 10 (for which $k_v(2) = 0.05$ md) is about 0.55 kg/s, whereas a simulation using $k_v(2) = 0.25$ md resulted in a net upflow of 1.4 kg/s. For values of caprock layer permeability exceeding about 0.25 md, the rate of drainage of liquid across this layer prevented the development of a vapor-dominated zone in our model. Conversely, for values of $k_v(2)$ less than about 0.05 m day the net rate of upflow from the vapor-dominated zone at quasi steady state becomes unre-

alistically low if pressures in the vapor-dominated zone are required to be in the range of 31–34 bars. Thus the range of values of caprock permeability for which a vapor-dominated zone could have evolved is reasonably well constrained.

As is noted above, the results illustrated in Figures 10 and 11 apply to mechanism 1, the increase in permeability of the lateral conduit. A slight variation of this mechanism that would yield similar results would be an increase in vertical permeability beneath the hot spring discharge boundary. Such a change in permeability could result from tectonic activity or glacial erosion. Because total simulation times are on the order of 10,000 years, these changes could take place gradually without significantly altering the quasi steady state results.

Simulations involving mechanism 2, a decrease in the inflow rate M, yielded results similar to those in Figures 10 and 11 except that quasi steady state conditions took about 25% less time to develop after drainage was initiated [*Ingebritsen*, 1983]. This was because the lateral conduit was effectively preheated during an initial period with both upflow and lateral outflow. A decrease in high-enthalpy inflow during the evolution of the Lassen system could have resulted from some combination of long-term changes in climate that caused a reduction in the rate of meteoric water recharge to the system, diminution in the conductive heat input from a cooling magma body which reduced fluid temperatures at depth and fluid density differences driving the circulation system, and sealing of flow conduits at depth due to mineral deposition or tectonic activity.

Mechanism 3, a lowering of the elevation at which high-chloride thermal water discharges, was not simulated, but may have been involved to some extent in the development of the part of the Lassen system beneath the glacially eroded Mill Creek Canyon. For glacial action to effect such a lowering the system must have been active before the end of the last major glacial period (10,000 years ago). This mechanism appears to have been effective in a related situation at the Valles Caldera, where high-chloride water discharges within the fault-controlled San Diego Canyon and travertine deposits on a granitic intrusive at Soda Dam are evidence of a gradual lowering of the elevation of hot-spring discharge by about 200 m (F. Trainer, personal communication, 1983).

Mechanism 4 does not involve any change in rock properties or boundary conditions; it involves only the decrease in fluid viscosity that occurs as the lateral conduit is heated by the flow of hot water away from the upflow region. As fluid viscosity decreases, the rate of flow in the lateral conduit tends to increase. Simulations using this mechanism did not yield the desired quasi steady state results, however, because the initial hydrostatic pressure distribution (for a sloping upper boundary) produces such a large lateral pressure gradient that almost all the specified mass inflow (M) flows out the lateral conduit. Consequently, flow rates within the upflow zone above the lateral conduit were too small to heat this region sufficiently for a vapor-dominated zone to form. Evidently, some change in rock properties and/or boundary conditions was necessary for the evolution of the Lassen hydrothermal system.

The Corey relative permeability functions were developed for problems involving two-phase flow through porous media and are commonly used in geothermal reservoir engineering analyses. Other functions that yield higher values of steam relative permeability may be more applicable to two-phase flow through fractured media because they yield greater values
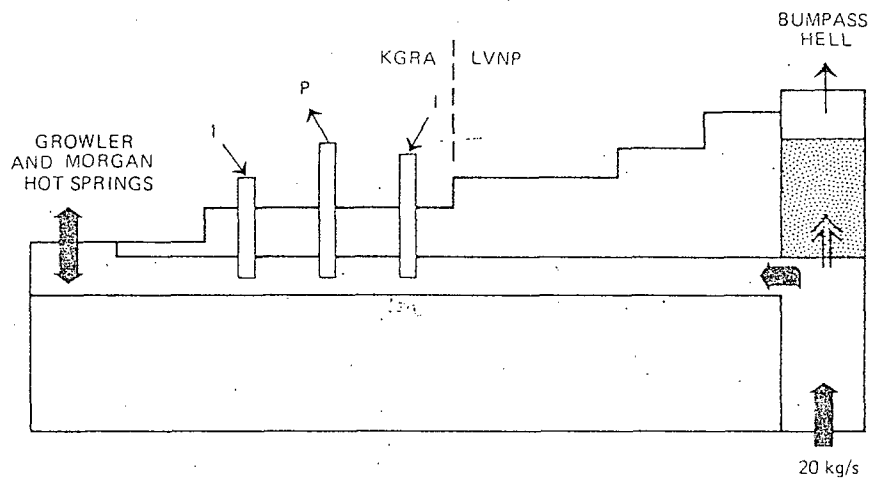
Fig. 12. Locations of production (P) and injection (I) wells used in simulations of the effects of geothermal development from a lateral conduit beneath Mill Creek Canyon. Arrows show direction of liquid flow (solid) and steam flow (open). Vapor-dominated zone shown by dotted pattern.

of steam relative permeability. Since the nature of the lateral outflow zone between Bumpass Hell and Growler and Morgan Hot Springs is not yet known, both the Corey functions and the "fracture-flow" functions of Sorey et al., [1980] were used in our simulations. The fracture-flow equations are

$$k_{rl} = [(S - 0.3)/0.65]^4$$

$$k_{rs} = [1 - k_{rl}]$$

The choice of relative permeability functions did not have a significant effect on long-term simulations of the evolution and natural state of the Lassen system but did have a impact on the simulated response of the system to geothermal development.

DEVELOPMENT SIMULATIONS

Simulations of geothermal development were also carried out with the geometric model representing the flow system between Bumpass Hell and Growler and Morgan Hot Springs (Figure 9b). This orientation includes the Mill Creek Canyon, perhaps the most likely target for geothermal exploration within the Lassen KGRA.

Quasi steady state results from four different cases were used as initial conditions for development. Two of these cases involved an extensive region of liquid-dominated two-phase flow in the lateral conduit, one for each of the two sets of relative permeability functions referred to previously, and two involved single-phase liquid flow in the conduit away from the region of phase separation, one for each of the relative permeability functions. An additional variable considered in the development simulations was the vertical permeability of the caprock layer above the vapor-dominated zone.

The results from the development simulations indicate that under certain conditions fluid production from lateral outflow conduits could alter the surficial discharge of thermal fluids within LVNP and the Lassen KGRA. The model used in these simulations is simplified, and if subsurface data were available for constructing a more detailed and realistic model, numerical simulations might be expected to show somewhat different results in terms of the timing and magnitude of effects. However, the results obtained with the present model concerning the type of induced changes and the conditions necessary for such changes are considered valid. Qualitatively, these

changes are similar to those observed at the Tauhara field, New Zealand in response to development at Wairaekei [Henley and Stewart, 1983].

Production-Injection Schemes

The production-injection scheme used in our simulations (Figure 12) consists of a production grid block centered 1.5 km outside the Park boundary and injection blocks centered 1 km upstream (towards the Park) and 1 km downstream from the production block.

Development simulations were carried out for production rates of 50, 100, and 250 kg/s, which correspond to electric power generation of about 5, 10, and 25 MW$_e$, respectively, for reservoir temperatures near 200°C. Results of these simulations are summarized in Table 2. Without reinjection, a production rate of 100 kg/s caused pressures in the production block to fall to less than a realistic cutoff point of 3 bars after periods of 11–21 years. This reflects limitations imposed by the permeability and cross-sectional area of the conduit.

A production rate of 250 kg/s could be sustained for nearly 40 years with reinjection at 80% of the production rate. For production rates greater than 250 kg/s with 80% reinjection, either production-block pressures fell below 3 bars or production-block temperatures declined from 200°C to less than a realistic cutoff point of 150°C within a period of 40 years. Temperature declines in the production block result from breakthrough of lower temperature water injected at 100°C or from induced recharge (at 10°C) across the constant pressure boundary at the left side of the model. In simulations with a reinjection rate equal to 100% of the production rate, pressures in the production block did not fall significantly, but the decline in production-block temperature was still a limiting factor.

Effects on Hot Springs in Lassen KGRA

During all of the development simulations, except for those with a reinjection rate equal to the production rate, the rate of fluid flow across the constant pressure boundary in the vicinity of Growler and Morgan Hot Springs changed (Table 2). Initially, approximately 20 kg/s discharged at this boundary. Depending upon the specified production-injection rates and the vertical permeability beneath the boundary ($k_z(1)$), the sim-

TABLE 2. Results of Development Simulations in Terms of Times Required for Pressures and Temperatures in the Production Block to Reach Limits of 3 Bars and 150°C, Respectively, and the Resultant Change in Discharge of the High-Chloride Hot Springs

Run	Production Rate, kg/s	Injection Rate, kg/s		$k_v(1)$, md*	Relative Permeability Functions	Time to Pressure Limit, yr	Time to Temperature Limit, yr	Hot Spring Discharge, kg/s†
		Upstream	Downstream					
1	50	0	0	100	Corey	>300	>300	−31
2	50	0	0	100	Fracture	>300	>300	−27
3	50	0	0	0.6	Corey	55	47	−1.6
4	50	0	0	0.6	Fracture	63	55	−2.3
5	50	0	40	100	Corey	>300	>300	9.5
6	50	0	40	0.6	Corey	>300	270	13
7	50	40	0	0.6	Corey	>300	240	11
8	50	0	50	0.6	Corey	>300	>300	20
9	50	50	0	0.6	Corey	>300	175	19
10	100	0	0	100	Corey	11	10	−40
11	100	0	0	100	Fracture	18	16	−50
12	100	0	0	0.6	Fracture	21	18	−2.2
13	100	80	0	0.6	Corey	>300	100	1.8
14	250	200	0	100	Corey	>300	36	−40
15	250	200	0	0.6	Corey	42	36	−1.9

Production block was centered 1.5 km south of Park boundary (Figure 12). Injection blocks were centered 0.5 km south of Park boundary (upstream) and 2.5 km south of Park boundary (downstream). Vertical permeability of caprock layer = 0.5 md for all runs listed. See text for forms of relative permeability functions.

*Vertical permeability of conduit beneath high-chloride hot springs. Horizontal permeability of lateral flow conduit = 140 md for runs with $k_v(1) = 100$ md and 180 md for runs with $k_v(1) = 0.6$ md.

†Flow rate across constant pressure boundary at left side of model. Negative sign indicates downflow. Value listed applies to a development time of 50 years or when the 3-bar pressure limit or the 150°C temperature limit was reached, whichever was smaller.

ulated flow at this boundary either decreased in magnitude or reversed direction in response to production. A reversal in direction corresponds to disappearance of hot spring discharge and induced recharge of cold water from the land surface. The simulated rate of induced recharge was greater and the pressure declines in the lateral conduit less for cases with a high value of $k_v(1)$ than for cases with a low value of $k_v(1)$.

If the southward trending lateral flow conduit actually extends further south than Morgan Hot Springs, induced "recharge" of thermal fluid from areas not included in our model could lessen, but not eliminate, the negative effects of fluid production on hot spring discharge. Locating high-temperature production areas south of Morgan Hot Springs seems unlikely in view of probable decreases in fluid temperature with distance from the Park.

Effects on Thermal Discharge in LVNP

Fluid production from the lateral conduit in our model causes pressure declines that tend to propagate both upstream (toward the Park) and downstream from the production area. The rates and magnitudes of pressure changes induced within portions of the conduit beneath LVNP vary significantly depending on the difference between the specified production and injection rates, the relative permeability functions used, and most significantly, the extent of two-phase conditions in the conduit before development starts. Under certain conditions the discharge of steam and steam condensate at the land surface above the central upflow area in LVNP could be noticeably affected by geothermal development outside the Park.

The plots in Figure 13 show variations in the net upflow of steam into and out of the vapor zone during selected development runs. These runs involved single-phase liquid conditions in the lateral conduit away from the central upflow

zone before development and production of 50 kg/s with no reinjection. They show the effects of varying the relative permeability functions and the vertical permeability of the caprock layer.

The temporary increases in steam upflow seen in these simulations are followed by decreases to levels at or below the initial flow rates. Pressures in the region of phase separation beneath the vapor-dominated zone decline throughout the development period. At early times, corresponding decreases in liquid saturation and increases in steam relative permeability dominate and cause the rapid rise in steam upflow. After 5–10 years, liquid saturation and steam relative permeability stabilize, and the continued pressure decline beneath the vapor-dominated zone causes the rate of steam upflow to decrease.

Changes in steam upflow are most pronounced for the case with fracture-flow relative permeability functions, where the increase in steam flow into the caprock amounts to about 32% of the initial flow rate. Changes in steam upflow were considerably smaller for run 3 and particularly run 1a. In run 1a the caprock permeability was increased by a factor of five to 0.25 md. Using the higher value of $k_c(2)$, the initial rate of steam upflow from the quasi steady state simulation is nearly twice the value for the lower $k_c(2)$ cases, but changes in net upflow during development are relatively subdued. This subdued response is partly due to the difference in the initial pressure-temperature distributions in the lateral conduit, which for run 1a involved less overpressure with respect to the corresponding saturation pressures than for run 3. The degree of overpressure affects the magnitude of pressure decline that can propagate from the production area before boiling occurs. In other respects, results for run 1a were similar to those listed in Table 2 for run 1.

Simulated changes in net steam upflow into the caprock were in all cases very small compared to the changes within
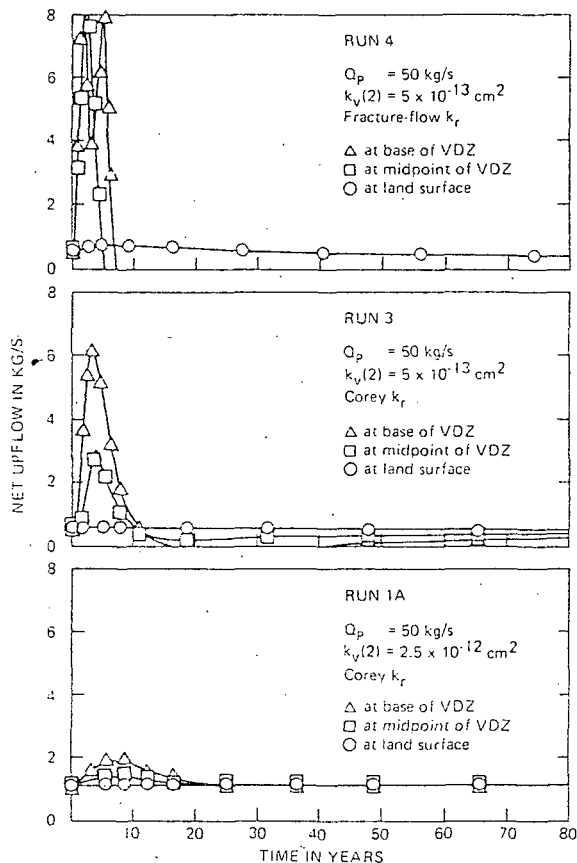
Fig. 13. Development simulations involving production rate Q_p without reinjection for cases with single-phase initial conditions in the lateral conduit. Production starts at 0 years and ceases if the pressure limit of 3 bars is reached (see Table 2 for additional details).

The distance L over which significant pressure changes (those 0.1 times the pressure change at the source) can propagate through a homogeneous reservoir in time t is given by

$$L = (tD)^{1/2} \qquad \text{radial flow}$$

$$L = 2(tD)^{1/2} \qquad \text{linear flow}$$

where $D = k/[n\mu_f(C_f + C_r)]$, D is hydraulic diffusivity, k is intrinsic permeability, n is porosity, μ_f is dynamic viscosity, C is compressibility, and the subscripts f and r refer to fluid and rock, respectively. These relationships can be derived from the appropriate line-source solutions for flow in radial and linear reservoirs with homogeneous properties. Although fluid properties were not constant in the numerical simulations, the relationship shown above for linear flow provides a qualitative basis for delineating the effects of two-phase fluid compressibility and reservoir properties on the transmission of induced pressure changes.

The effective fluid compressibility under two-phase conditions is approximately 4 orders of magnitude greater than the compressibility of liquid water [Grant and Sorey, 1979]. Hence as is noted above, the effects of fluid production propagate much smaller distances through boiling fluid than through liquid in a given time period. Data on reservoir permeability and porosity are obviously required to determine the actual speed at which induced pressure changes would propagate under LVNP. Our simulations can only constrain the permeability area product for the southward trending lateral flow zone. If the actual cross-sectional area of the conduit is smaller and the permeability larger than assumed in our model, or if the porosity is lower than assumed, the rate of transmission of pressure changes induced by production would be faster.

Reinjection

Reinjection of produced fluids (or injection of water from another source) is often cited as a means for protecting surficial discharge features from the effects of geothermal development. Our results indicate that such protection is possible, but may be difficult to achieve. As is discussed above, an injection rate equal to the production rate was required to avoid diminution in the flow of hot springs located downstream from the production area in our simulations. However, with either upstream or downstream injection at rates equal to the production rates, simulated pressure changes tended to propagate upstream under the Park (Figure 14a). Injection of 100% of produced fluid downstream from the production block was accompanied by pressure declines at all grid blocks to the right of the injection block, resulting in the same type of response in the vapor-dominated zone as is shown in Figure 13. In contrast, the same rate of fluid injection upstream from the production block caused a pressure rise to propagate under the Park, resulting in a sharp decrease in steam upflow owing to increased liquid saturation beneath the vapor-dominated zone.

For injection rates equal to 80% of production rates (Figure 14b), pressures in the lateral conduit under the Park were lowered, regardless of whether fluid was injected upstream or downstream of the production zone. These results suggested, however that upstream injection of between 80 and 100% of the produced fluid could minimize or eliminate induced pressure changes in the lateral conduit beneath the Park. This percentage might change with time, as the temperature changes associated with production and injection affect fluid mobility in the lateral conduit. In the case illustrated in Figure

and below the vapor-dominated zone. Although increases in the steam upflow rate are partially damped within the vapor zone itself by condensation and accompanying pressure rises, this primarily reflects the low value of vertical permeability applied to the caprock layer. As the value of $k_v(2)$ is increased, the ratio of change in steam upflow into the caprock to change in steam upflow at the base of the vapor-dominated zone increases. As is noted above, relatively low values of caprock permeability appear to have been necessary to allow a vapor-dominated zone to evolve. However, it is possible that higher-permeability channels could have developed after the vapor-dominated zone was established, perhaps due to solution of rock minerals by the chemically active condensate [D'Amore and Truesdell, 1979]. A more detailed model that includes separate channels for steam and liquid flow above the vapor-dominated zone is required to adequately quantify the magnitude of changes in steam flow at the land surface induced by geothermal development.

Although boiling and two-phase flow are induced in and near the production area in runs in which the lateral conduit is initially single phase, the drop in pressure to saturation values for the initial temperatures is transmitted relatively rapidly and hence can reach the central upflow zone during the development period. If the lateral conduit initially contains an extensive region of liquid-dominated two-phase flow (runs listed in Table 2 with $k_u(1) = 100$ md), the simulated effects of fluid production do not propagate as far back as the central upflow zone because of the high effective fluid compressibility in the two-phase portion of the lateral conduit [Grant and Sorey, 1979].
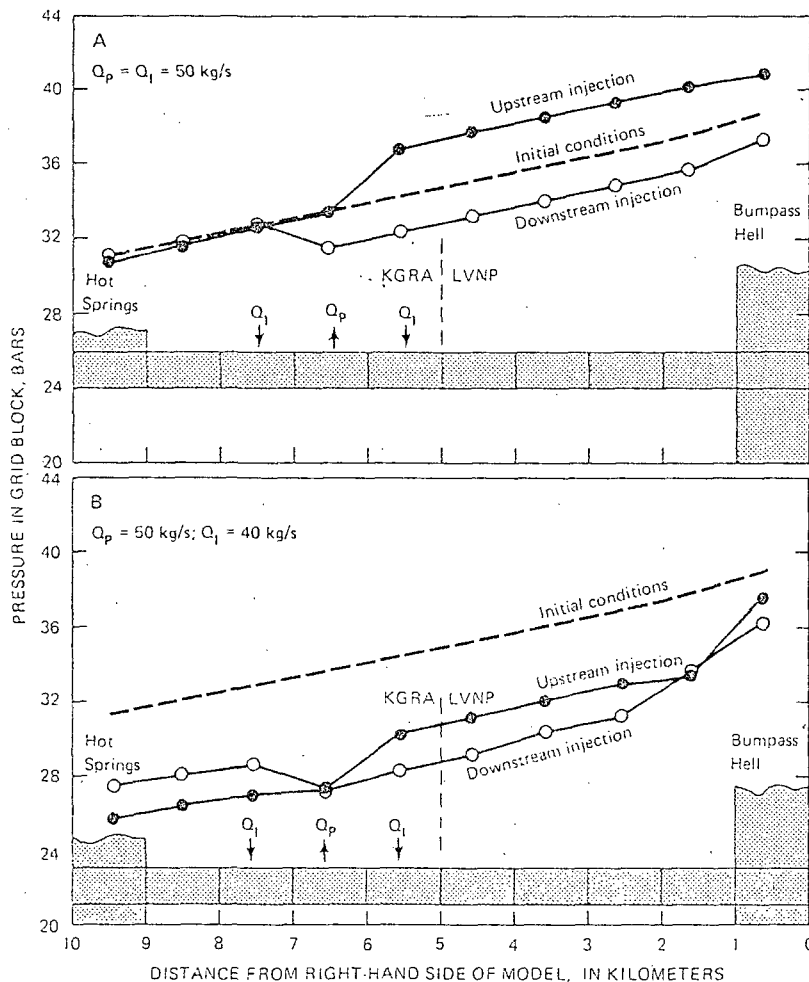
Fig. 14. Plots of grid-block pressures within the lateral conduit for development simulations involving production from the grid block with the black arrow and injection into the grid block to the right of the production block for the upstream injection case and into the grid block to the left of the production block for the downstream case. Results apply to a development time of approximately 40 years.

14, a constant reinjection rate equal to 89% of production (44.5 kg/s) leaves pressures beneath the Park essentially unchanged after 40 years.

Further experimentation with a combination of upstream and downstream reinjection showed that upstream reinjection at 30% of the production rate (15 kg/s) combined with downstream reinjection at 70% of the production rate (35 kg/s) also left pressures beneath the Park unchanged after 40 years. In addition, because the total injection rate is equal to the production rate, this production-injection scheme maintains the flow of hot springs downstream from the production area.

CONCLUSIONS

Existing data support a conceptual model of the Lassen hydrothermal system in which boiling and phase separation occur within a central upflow zone beneath Bumpass Hell, giving rise to an upflow of steam through a parasitic vapor-dominated zone and lateral flow of liquid toward discharge areas outside LVNP. The simplest model accounting for the distribution of areas of steam and steam-heated discharge within LVNP and areas of discharge of high-chloride thermal water in the Lassen KGRA involves lateral outflow of thermal water along two orientations, one leading southward from Bumpass Hell to Growler and Morgan Hot Springs in Mill Creek Canyon and the other leading southeastward to Terminal Geyser and Domingo Spring. Quantitative constraints on this conceptual model include estimates of temperature and

pressures in a central vapor zone of 235°–240°C and 31–34 bars, and estimates of the lateral outflow of thermal water in Mill Creek Canyon and at Domingo Spring of 17 and 2.7 L/s, respectively.

Numerical simulations of heat and fluid flow in a two-dimensional vertical cross-section representing the Bumpass Hell to Growler and Morgan Hot Springs axis indicate that the present-day Lassen hydrothermal system could have evolved from an early period of upflow and convective heating by several processes that initiate a period of lateral outflow at rates greater than the rate of upflow from depth, and consequently, cause liquid to drain from beneath a low-permeability caprock layer. Although formation of a thick parasitic vapor-dominated zone could take place in less than 1,000 years, much longer times are required for temperatures within the lateral outflow conduit to stabilize. From the evolution simulations, a value for the permeability-thickness product of a 1-km-wide lateral conduit beneath Mill Creek Canyon of approximately 32 Darcy meters can be estimated, assuming a total through-flow rate of 20 kg/s.

The effects of fluid production for geothermal development from the lateral conduit beneath Mill Creek Canyon were simulated for production rates of 50-250 kg/s, with and without reinjection at 80 and 100% of the production rates. Production with less than 100% reinjection is likely to cause a diminution in the discharge of thermal water in Mill Creek Canyon and possibly a reversal from upflow of hot water to

downflow of cold water. Our simulations also indicate that in the absence of a carefully planned reinjection scheme, thermal discharge features within LVNP could be affected by geothermal development outside the Park if fluid flow within the lateral outflow conduits is initially single-phase liquid. In this case pressure declines would propagate relatively rapidly to the central upflow area within LVNP, causing a temporary increase and subsequent decrease in the rate of steam upflow.

References

Allis, R. G., Possible effects of reinjection at Wairaekei geothermal field, *Geotherm. Res. Counc. Trans.*, *4*, 389–392, 1980.

Beall, J. J., A hydrologic model based on deep test data from the Walker "O" No. 1 well, Terminal Geyser, California, *Geotherm. Res. Counc. Trans.*, *5*, 153–156, 1981.

Christopherson, K. R., and L. Pringle, Additional audiomagnetotelluric soundings in the Lassen Known Geothermal Resources Area, Plumas and Tehama Counties, California, *U.S. Geol. Surv. Open File Rep.*, *81–959*, 18 pp., 1981.

Clynne, M. A., The stratigraphy and major element geochemistry of the Lassen volcanic center, M.S. thesis, 155 pp., San Jose State Univ., Calif., 1983.

D'Amore, F., and C. Panichi, Evaluation of deep temperatures of hydrothermal systems by a new gas geothermometer, *Geochim. Cosmochim. Acta*, *44*, 549–556, 1980.

D'Amore, F., and A. H. Truesdell, Models for steam chemistry at Larderello and The Geysers, paper presented at the Fifth Workshop on Geothermal Reservoir Engineering, Stanford University, Stanford, Calif., 1979.

Faust, C. R., and J. W. Mercer, Geothermal reservoir simulation, 2, Numerical solution techniques for liquid- and vapor-dominated hydrothermal systems, *Water Resour. Res.*, *15*, 31–46, 1979.

Fenneman, N. M., Physiographic division of the United States, *Ann. Assoc. Am. Geogr.*, *18*, 261–353, 1928.

Friedman, J. D., and D. Frank, Thermal surveillance of active volcanoes using the Landsat-1 data collection system, 4, Lassen volcanic region, Final report, 46 pp., Goddard Space Flight Center, Greenbelt, Md., 1978.

Grant, M. A., Intepretation of downhole pressure measurements at Baca, paper presented at the Fifth Workshop on Geothermal Reservoir Engineering, Stanford University, Stanford, Calif., 1979.

Grant, M. A., and M. L. Sorey, The compressibility and hydraulic diffusivity of steam-water flow, *Water Resour. Res.*, *15*, 684–686, 1979.

Heiken, G., and J. C. Eichelberger, Eruptions at Chaos Crags, Lassen Volcanic National Park, California, *J. Volcan. Geotherm. Res.*, *7*, 443–481, 1980.

Henley, R. W., and M. K. Stewart, Chemical and isotopic changes in the hydrology of the Tauhara geothermal field due to exploitation at Wairaekei, *J. Volcanol. Geothermal Res.*, *15*, 285–314, 1983.

Hubbert, M. K., Entrapment of petroleum under hydrodynamic conditions, *Am. Assoc. Pet. Geol. Bull.*, *21*, 1945–2026, 1953.

Ingebritsen, S. E., Evolution of the geothermal system in the Lassen Volcanic National Park area, M.S. thesis, 90 pp., Stanford Univ., Calif., 1983.

Ingebritsen, S. E., and S. A. Rojstaczer, The Sifford Peak Rings: A late Pliocene nested caldera complex? (abstract), *Eos Trans. AGU*, *64*, 879, 1983.

Janik, C. J., N. L. Nehring, and A. H. Truesdell, Isotope geochemistry of thermal fluids from Lassen Volcanic National Park, *Geotherm. Res. Counc. Trans.*, *7*, 295–300, 1983.

Mase, C. W., J. H. Sass, and A. H. Lachenbruch, Near-surface hydrothermal regime of the Lassen "Known Geothermal Resources Area," California, *U.S. Geol. Surv. Open File Rep.*, *80-1230*, 18 pp., 1980.

Muffler, L. J. P., N. L. Nehring, A. H. Truesdell, C. J. Janik, M. A. Clynne, and J. M. Thompson, The Lassen geothermal system, paper presented at the Pacific Geothermal Conference, University of Auckland, Auckland, New Zealand, 1982.

Nehring, N. L., R. H. Mariner, D. L. White, M. A. Huebner, E. D. Roberts, K. Haron, P. A. Bowen, and L. Tanner, Sulphate geothermometry of thermal waters in the western United States, *U.S. Geol. Surv. Open File Rep.*, *79-1135*, 5 pp., 1979.

Sorey, M. L., and S. E. Ingebritsen, Evolution of liquid-dominated hydrothermal systems with parasitic vapor-dominated zones, paper presented at the Fifth New Zealand Geothermal Workshop, University of Auckland, Auckland, New Zealand, 1983a.

Sorey, M. L., and S. E. Ingebritsen, Numerical simulations of the hydrothermal system at Lassen Volcanic National Park, paper presented at the Ninth Workshop on Geothermal Reservoir Engineering, Stanford University, Stanford, Calif., 1983b.

Sorey, M. L., and S. E. Ingebritsen, Quantitative analysis of the hydrothermal system in Lassen Volcanic National Park and Lassen KGRA, *U.S. Geol. Surv. Water Res. Invest. Rep.*, *84-4278*, 80 pp., 1984.

Sorey, M. L., M. A. Grant, and E. Bradford, Nonlinear effects in two-phase flow to wells in geothermal reservoirs, *Water Resour. Res.*, *16*, 767–777, 1980.

Thompson, J. M., Chemical analyses of thermal and nonthermal springs in Lassen Volcanic National Park and vicinity, California, *U.S. Geol. Surv. Open File Rep.*, *83-311*, 23 pp., 1983.

White, D. E., L. J. P. Muffler, and A. H. Truesdell, Vapor-dominated hydrothermal systems compared with hot-water systems, *Econ. Geol.*, *66*, 75–97, 1971.

S. E. Ingebritsen and M. L. Sorey, U.S. Geological Survey, 345 Middlefield Road, Menlo Park, CA 94025.